Brain Stimulation 7 (2014) 603–607

Contents lists available at ScienceDirect

Brain Stimulation

journal homepage: www.brainstimjrnl.com

Subthalamic Nucleus Deep Brain Stimulation Induces Motor Network BOLD Activation: Use of a High Precision MRI Guided Stereotactic System for Nonhuman Primates☆

Hoon-Ki Min [a,b,c,1], Erika K. Ross [a,1], Kendall H. Lee [a,b,*], Kendall Dennis [c], Seong Rok Han [a,d], Ju Ho Jeong [a,e], Michael P. Marsh [a], Bryan Striemer [f], Joel P. Felmlee [f], J. Luis Lujan [a,b,c], Steve Goerss [a], Penelope S. Duffy [a], Charles D. Blaha [g], Su-Youne Chang [a,b], Kevin E. Bennet [a,c]

[a] Department of Neurologic Surgery, Mayo Clinic, Rochester, MN, USA
[b] Department of Physiology and Biomedical Engineering, Mayo Clinic, Rochester, MN, USA
[c] Division of Engineering, Mayo Clinic, Rochester, MN, USA
[d] Department of Neurosurgery, Ilsan Paik Hospital, College of Medicine, Inje University, Goyang, Republic of Korea
[e] Department of Neurosurgery, Kosin University Gospel Hospital, Busan, Republic of Korea
[f] Department of Radiology, Mayo Clinic, Rochester, MN, USA
[g] Department of Psychology, University of Memphis, Memphis, TN, USA

ARTICLE INFO

Article history:
Received 30 January 2014
Received in revised form
19 April 2014
Accepted 25 April 2014
Available online 3 June 2014

Keywords:
Deep brain stimulation
Subthalamic nucleus
Functional magnetic resonance imaging
Nonhuman primate
Motor cortex
Pedunculopontine nucleus

ABSTRACT

Background: Functional magnetic resonance imaging (fMRI) is a powerful method for identifying *in vivo* network activation evoked by deep brain stimulation (DBS).
Objective: Identify the global neural circuitry effect of subthalamic nucleus (STN) DBS in nonhuman primates (NHP).
Method: An in-house developed MR image-guided stereotactic targeting system delivered a mini-DBS stimulating electrode, and blood oxygenation level-dependent (BOLD) activation during STN DBS in healthy NHP was measured by combining fMRI with a normalized functional activation map and general linear modeling.
Results: STN DBS significantly increased BOLD activation in the sensorimotor cortex, supplementary motor area, caudate nucleus, pedunculopontine nucleus, cingulate, insular cortex, and cerebellum (FDR < 0.001).
Conclusion: Our results demonstrate that STN DBS evokes neural network grouping within the motor network and the basal ganglia. Taken together, these data highlight the importance and specificity of neural circuitry activation patterns and functional connectivity.

Introduction

Deep brain stimulation (DBS) has been shown to be an effective treatment option for movement disorders including Parkinson's disease (PD) [1]. Although the mechanisms of stimulation-induced neuromodulation are not completely understood, it is known that modification of given brain functions by DBS depends on targeting specific sites in the complex neuronal circuitry underlying disease state dysfunction [2–4].

There has been increasing interest in using functional imaging to investigate the global brain effects of subthalamic nucleus (STN) DBS in PD patients [5–9]. To characterize the functional neural network of DBS, our group previously developed a method for functional magnetic resonance imaging (fMRI) in a swine model of DBS [10–12].

Given that the STN is a key relay area in the basal ganglia (BG)–thalamocortical circuitry [13], the sensorimotor subregion of the STN has become the clinical DBS target for PD [14]. Thus, the importance of precise targeting within the STN and the induced functional network effects on the BG and cortical circuitry by high frequency stimulation warrants examination.

Here, we describe a novel stereotactic system that facilitates miniature DBS electrode implantation in the nonhuman primate (NHP). To increase targeting precision in the small and irregularly

This work was supported by the National Institutes of Health (R01 NS 70872 awarded to KHL) and by The Grainger Foundation.
Financial disclosure: The authors declare no competing financial interests.
* Corresponding author. Mayo Clinic, 200 First Street SW, Rochester, MN 55905, USA.
E-mail address: lee.kendall@mayo.edu (K.H. Lee).
[1] These authors contributed equally to this work.

1935-861X/$ – see front matter © 2014 The Authors. Published by Elsevier Inc. All rights reserved.
http://dx.doi.org/10.1016/j.brs.2014.04.007

shaped STN, this system was designed with an orthogonal coordinate system (X, Y, Z, arc, and collar) using an arc system similar to that of clinical stereotactic systems [15]. Using this system, we were able to identify specific global functional neural network and circuitry effects induced by STN DBS in normal NHP.

Materials and methods

Animals and surgical procedure

Study procedures were performed in accordance with the National Institutes of Health Guidelines for Animal Research (Guide for the Care and Use of Laboratory Animals) and approved by the Mayo Clinic Institutional Animal Care and Use Committee (IACUC). The subject group consisted of two male rhesus macaques (*Macaca mulatta*) weighing 7 ± 1 kg. Sedation was maintained with 1.75–2.5% isoflurane during surgery and 1.5%–1.75% during the fMRI experiment. Vital signs were continuously monitored throughout the procedures.

An MR image-guided stereotactic targeting system specifically developed by our group for NHP, was used for stimulating electrode targeting and implantation (Supplementary Fig. S1A). A miniature Platinum–Iridium DBS electrode consisting of six cylindrical contacts (625 μm in diameter and 500 μm in length) separated by 500 μm (NuMed, Inc.) was introduced to the right hemisphere STN. Imaging was conducted by a 3 T MR scanner (Signa HDx, General Electric) with a custom, in-house designed four-channel phased array radiofrequency coil (Mayo Clinic). A T1-weighted 3D magnetization prepared rapid gradient echo (MP-RAGE) and T2-weighted 2D fast spin echo (FSE) (Supplementary Table S1) were used to identify the STN, based on the Rhesus Macaque brain atlas [16] and anatomical landmarks (e.g., red nucleus in the axial view) in the MR image (see Supplementary Figs. S1 and S3 for coordinate details). Electrode location was confirmed by x-ray fluoroscopy (SIREMOBIL Compact, Siemens AG) during surgery and by 3D computer tomography (CT) (Dual source Somatom Definition, Siemens AG) postoperatively (Supplementary Fig. S1D).

Functional MRI during DBS

Following two to four weeks of post-surgical recovery, fMRI experiments were conducted using a gradient echo (GRE) echo-planar imaging (EPI) pulse sequence (integrated spatial spectral pulse for fat suppression) with an anatomical 2D T2-weighted GRE image (Supplementary Table 1). Based on the MRI-CT fusion image, the selected stimulation contacts included the medial to dorsolateral portion of the STN and zona incerta area (Supplementary Fig. S3). The electrical stimulation parameters were biphasic 5 V pulses at 130 Hz and pulse widths of 150 μs (A-M systems, Model 2100 isolated pulse stimulator). An event-related-like block design was used to detect putative BOLD signal responses evoked by electrical stimulation, performing five stimulus/rest blocks (6 s ON/60 s OFF). Two fMRI experiments were performed on each subject, resulting in a total four fMRI data sets that were conducted on four separate days ($n = 2$, data set $= 4$). The stimulating electrode was not active between imaging sessions.

Data processing and analysis

A standard pre-processing sequence, including slice scan time correction, 3D motion correction, temporal filtering, and spatial smoothing (Gaussian filter with FWHM: 1.3 pixel size) was applied to each data set (Brain Innovation, BrainVoyager QX). Double-gamma hemodynamic response function (onset 0 s, time to response peak 5 s, time to undershoot peak 15 s) correlated voxel-wise BOLD signal changes with the given stimulus protocol. To visualize the group BOLD pattern, the fMRI dataset was normalized to one subject's brain using a nonlinear co-registration based on the anterior and posterior commissure points and six boundaries of the brain (anterior, posterior, superior, inferior, right and left borders) using each subject's 3D MP-RAGE image (Brain Innovation, BrainVoyager QX). These datasets were further analyzed using linear regression analysis with the general linear model and multi-subject analysis. To correct for multiple comparisons and exclude false positive voxels, we considered only voxels with a False Discovery Rate (FDR) significance level

Table 1
Areas of significant brain activation.

	Location	Cluster size (mm)	Coordinates (x, y, z)	Max *t*-score	Possible circuits involved
130 Hz, 5 V, 0.15 ms	Cerebellum (C)	2019	−5, −7, 15	**16.47**[a]	Motor cortex-cerebellum connection, DS of cerebello-thalamic fibers
	Primary motor cortex (I)	487	4, 9, 38	**9.22**[a]	BGTC loop (Indirect pathway), Antidromic STN-Cortex, DS of CST in IC
	Primary somatosensory cortex (I)	607	26, 19, 16	**8.66**[a]	BGTC loop (Indirect pathway), Antidromic STN-Cortex, DS of CST in IC
	Cingulate cortex (I, C)	59	−3, 7, 32	**7.36**[a]	Limbic territory of STN
	Auditory cortex/Parietal operculum (C)	199	22, 3, 30	**6.50**[a]	Sensory input
	Caudate nucleus (I)	79	6, 27, 16	5.97	STN-SNc, DS of SN, DS of NSF, PPN-SNc
	Periaqueductal gray (I)	45	2, 2, 12	5.75	N/A
	Putamen (I)	18	8, 22, 16	5.58	STN-SNc, DS of SN, DS of NSF, PPN-SNc
	Supplementary motor area (C)	28	−2, 18, 31	5.46	BGTC loop (Indirect pathway), Antidromic STN-Cortex, DS of CST in IC
	Parahippocampal gyrus (I)	20	14, 2, 7	5.37	Limbic territory of STN
	Pedunculopontine nucleus (I)	29	3, 3, 7	5.37	STN-PPN
	Primary motor cortex (C)	33	−16, 15, 29	5.00	BGTC loop (Indirect pathway), Antidromic STN-Cortex, DS of CST in IC
	Medial lemniscus (I)	6	5, 2, 6	4.91	Sensory input
	Cerebellum (I)	13	17, −5, 7	4.78	Motor cortex-cerebellum connection, DS of cerebello-thalamic fibers
	Insular cortex (I)	8	19, 15, 18	4.50	Limbic territory of STN
	Caudate nucleus (C)	30	−8, 22, 19	−4.76	STN-SNc, DS of SN, DS of NSF, PPN-SNc
	Ventral lateral thalamic nucleus (C)	34	−6, 15, 20	−5.15	BGTC loop (Indirect pathway), Antidromic STN-CmPf, DS of thalamus
	Putamen (C)	35	−16, 23, 14	−5.27	STN-SNc, DS of SN, DS of NSF, PPN-SNc
	Amygdala (C)	84	−11, 22, 5	−5.83	Limbic territory of STN

Coordinates (mm): x = mediolateral, y = rostrocaudal, and z = dorsoventral. Abbreviations: BGTC, Basal ganglia-thalamocortical; C, Contralateral; CST, Corticospinal tract; DS, Direct stimulation through electric spread; I, Ipsilateral; IC, Internal capsule; NSF, Nigrostriatal fiber; PPN, Pedunculopontine nucleus; SNc, Substantia Nigra pars compacta; STN, Subthalamic nucleus.
Values in bold signifies FDR < 0.01.
[a] Areas showing with Bonferroni correction $P < 0.001$.

of <0.001 as representing sites of activation (Table 1). In addition to and separate from the FDR, we applied the more stringent Bonferroni correction (<0.001) to the original data. The brain areas that survived Bonferroni correction are listed in Table 1. To measure event-related BOLD response (BOLD signal/5 volume average of baseline), regions of interest (ROI) were selected from the normalized group data based on the brain atlas [16]. Factor analysis based on principal component analysis (PCA) with varimax rotation of the correlation matrix was performed on the ROI followed by k-means clustering of the three-dimensional Eigen plot (IBM Co., Statistical Package for the Social Sciences, version 20, IBM) [10].

Results

We designed and fabricated a stereotactic head frame to investigate DBS-induced functional activation in the NHP. Sub-millimeter

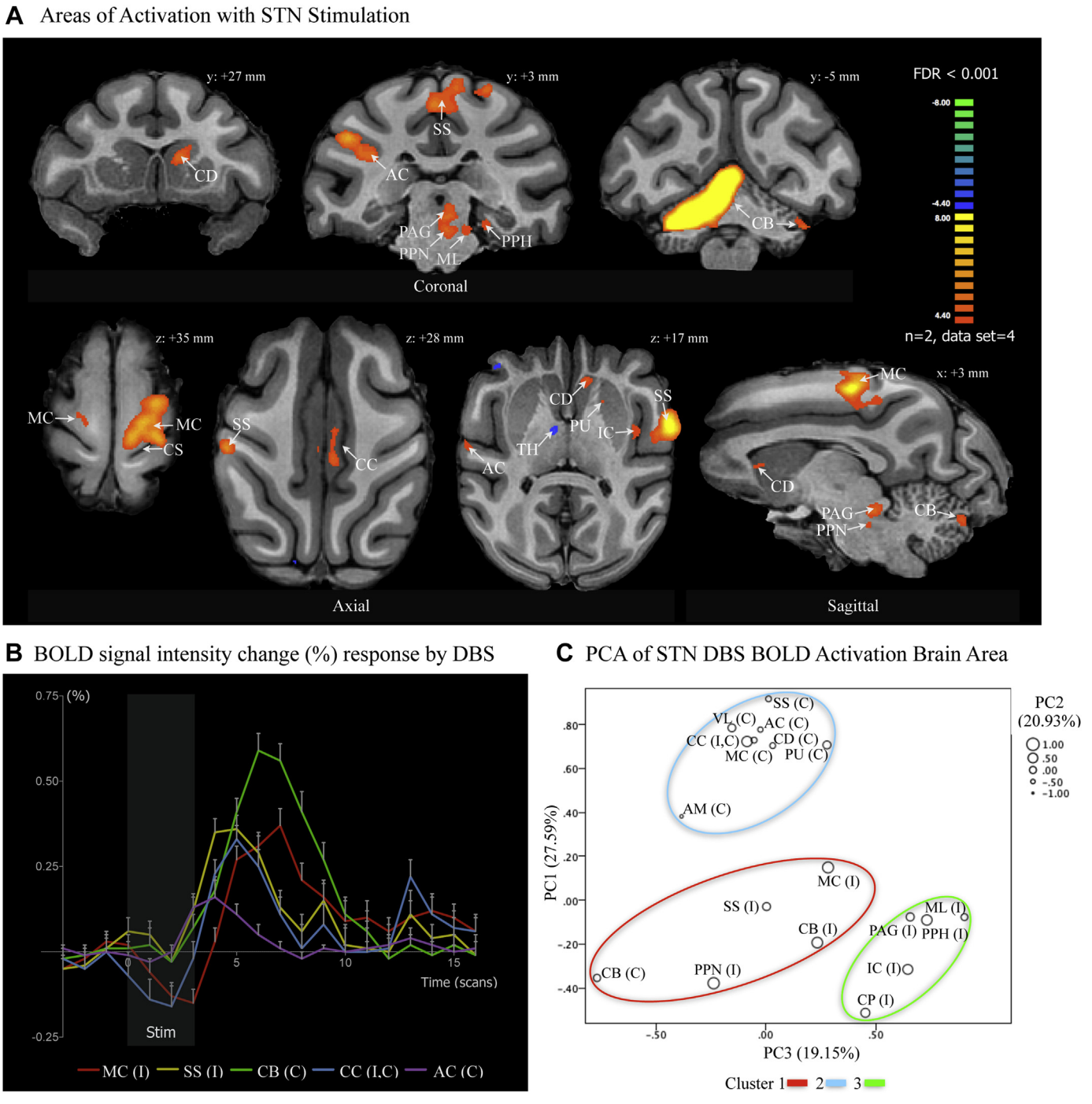

Figure 1. STN DBS (5 V, 130 Hz, and 150 μs). (A) Areas of activation with STN stimulation ($n = 2$, data set = 4); (B) Event-related BOLD percent change during and after STN DBS. Error bars represent standard error; (C) Principal component analysis between functionally defined regions of interest for STN DBS. Abbreviations: AC, auditory cortex; AM, amygdala; BOLD, blood oxygen level-dependent; C, contralateral; CB, cerebellum; CC, cingulate cortex; CD, caudate nucleus; CP, caudate nucleus and putamen; CS, central sulcus; DBS, deep brain stimulation; FDR, false discovery rate; I, ipsilateral; IC, insular cortex; MC, primary motor cortex; ML, medial lemniscus; PAG, pariaqueductal gray; PC, principal component; PCA, principal component analysis; PPH, parahippocampal gyrus; PPN, pedunculopontine nucleus; PU, putamen; SS, primary somatosensory cortex; Stim, stimulation; STN, subthalamic nucleus; TH, thalamus; VL, ventral lateral thalamic nucleus.

accuracy (dx = 0.30 ± 0.08, dy = 0.49 ± 0.16, dz = 0.76 ± 0.06 mm) was achieved in the final stereotactic targeting phantom test (see Supplementary Information and Fig. S2). The combined, concurrent fMRI – STN DBS (5 V, 130 Hz, and 150 μs) experiment revealed significant BOLD activation in the sensorimotor network, including primary motor cortex (MC), primary somatosensory cortex, supplementary motor area (SMA), the pedunculopontine nucleus (PPN) and the cerebellum (FDR < 0.001) with the contralateral cerebellum showing the highest *t*-score (see Fig. 1A and Table 1). The sensorimotor network results remained significant even after Bonferroni correction ($P < 0.001$ (Table 1)).

Areas of activation were also found in the BG circuitry, including the caudate nucleus and putamen. STN DBS also affected the contralateral MC, SMA, cingulate, caudate nucleus, putamen, ventral lateral thalamic nucleus, amygdala, and auditory cortex/parietal operculum. Of note, several of these contralateral areas including the caudate nucleus, putamen, ventral lateral thalamic nucleus, and amygdala showed negative BOLD response (Table 1). Limbic circuitry BOLD response was evoked in bilateral cingulate cortex, ipsilateral parahippocampus, insular cortex, and contralateral amygdala. Additional areas of sensory activation included the auditory cortex, the parietal lobe, and the medial lemniscus. Fig. 1B shows event-related time courses of BOLD percent changes with delayed hemodynamics peaking at 8–14 s in brain areas evoked by STN DBS. The ipsilateral primary motor cortex and bilateral cingulate cortex showed initial negative signal in the BOLD change.

Factor analysis was performed to identify jointly varying patterns of correlation among the eighteen ROIs (Fig. 1C). The PCA and subsequent cluster analysis revealed the following three distinct clusters associated with STN DBS ($P < 0.001$): a) Cluster 1: ipsilateral primary motor cortex, primary sensory cortex, pedunculopontine nucleus (PPN) and bilateral cerebellum; b) Cluster 2: contralateral primary motor cortex, primary sensory cortex, ventral lateral thalamic nucleus, caudate nucleus, putamen, amygdala, auditory cortex, and bilateral cingulate cortex; and c) Cluster 3: ipsilateral caudate nucleus, putamen, insular cortex, periaqueductal gray, parahippocampal gyrus, and medial lemniscus.

Discussion

There is increasing evidence that DBS modulation of the disease state is based on a circuitry effect related to the target stimulation area. This concept is supported by preclinical and clinical electrophysiological studies of DBS in movement disorders and psychiatric disease [2,4,17,18]. While region-specific DBS mechanisms have been investigated using electrophysiology and electrochemistry, the complex, dense wiring of the brain makes it extremely challenging to understand neuronal communication beyond a few synapses. Functional brain imaging has the advantage of providing global assessment of simultaneous neural activity.

We previously reported that STN DBS induced non-specific BOLD responses in both motor and non-motor networks in swine [10]. In the current study, we used a miniature DBS electrode to stimulate the medial-dorsal portion of the STN in an NHP model of DBS to further explore global functional circuitry effects.

Our results support clinical studies of human PD patients using fMRI, single-photon emission computed tomography (SPECT), and positron emission tomography (PET) during STN DBS. These studies report activation in ipsilateral primary sensorimotor cortex, premotor cortex, SMA, dorsolateral prefrontal cortex, BG, insular cortex, and contralateral cerebellum [7,8,19–21].

In addition, recent studies suggest that STN DBS might have a role in modulating cortical activity by normalizing the intracortical inhibitory mechanism [18,22]. A regional cerebral blood flow (rCBF) PET study showed that when effective STN stimulation was delivered during a movement task, motor areas were recruited, and there was also a widespread "normalization" of activity in primary motor cortex, SMA, and BG compared to the control group [23]. A rCBF SPECT study reported a correlation between improved motor scores and an increase in rCBF in the pre-SMA and primary motor cortex [9].

Recent optogenetic and cortical evoked potential studies suggest that the therapeutic effects of STN DBS may be induced by the modulation of select afferent neuronal populations projecting to the STN [24,25]. The direct antidromic activation of the motor cortex through the motor cortex-to-STN hyperdirect pathway [26,27] has been mentioned as contributing to the therapeutic effect of DBS in PD animal studies [27,28]. The contralateral STN DBS effect in our results may be indicative of the antidromic effects on the bilateral afferent cortical projections associated with this circuitry [29–31]. However, further study is needed to understand the effects of negative BOLD in the contralateral hemisphere.

To investigate the pattern of relationships among the activated brain areas, factor analysis revealed three distinct patterns of correlation among functionally defined ROIs. Cluster 1 consisted of brain areas that are predominantly in the ipsilateral motor network. Cluster 2 consisted mainly of contralateral brains areas, and Cluster 3 consisted mainly of the basal ganglia and limbic components.

Functional mapping of DBS is also important in that the sporadic cognitive/psychiatric complications of STN DBS have been attributed to current spread into adjacent neuronal structures [32–34]. Recent clinical studies indicate that there is a distinct relationship between specific electrode location within the STN and the corresponding therapeutic outcome [35,36]. Our finding of predominant activation in motor networks with associated limbic activation might be attributed to current spread into ventral STN and nearby associated regions [37,38].

Of note, the activation of PPN in both the NHP results reported here as well as in our previous swine models [10] suggest the importance of PPN in reduced gait freezing with STN DBS [39,40].

Using broad stimulation contact coverage with large current spread effects, the present study allowed us to estimate the maximum circuitry effect induced by STN DBS and thus to establish a proof-of-principle setup for future more refined circuitry studies. Despite the limitations of the anesthetized and non-disease state of our subjects, our results reveal neural network grouping within the motor network and the BG by STN DBS and highlight the importance of their specific neural circuitry activation patterns and functional connectivity. This study demonstrates an effective technique for both surgical targeting and functional network mapping for DBS in nonhuman primates.

Acknowledgments

We thank the Center for Advanced Imaging Research, Opus Building, Mayo Clinic for their support.

Supplementary data

Supplementary data associated with this article can be found, in the online version, at http://dx.doi.org/10.1016/j.brs.2014.04.007.

References

[1] Benabid AL. Deep brain stimulation for Parkinson's disease. Curr Opin Neurobiol 2003;13(6):696–706.
[2] Kringelbach ML, Jenkinson N, Owen SL, Aziz TZ. Translational principles of deep brain stimulation. Nat Rev Neurosci 2007;8(8):623–35.
[3] Lee KH, Blaha CD, Garris PA, Mohseni P, Horne AE, Bennet KE, et al. Evolution of deep brain stimulation: human electrometer and smart devices supporting the next generation of therapy. Neuromodulation 2009;12(2):85–103.
[4] McIntyre CC, Hahn PJ. Network perspectives on the mechanisms of deep brain stimulation. Neurobiol Dis 2010;38(3):329–37.

[5] Jech R, Urgosik D, Tintera J, Nebuzelsky A, Krasensky J, Liscak R, et al. Functional magnetic resonance imaging during deep brain stimulation: a pilot study in four patients with Parkinson's disease. Mov Disord 2001;16(6):1126–32.
[6] Stefurak T, Mikulis D, Mayberg H, Lang AE, Hevenor S, Pahapill P, et al. Deep brain stimulation for Parkinson's disease dissociates mood and motor circuits: a functional MRI case study. Mov Disord 2003;18(12):1508–16.
[7] Phillips MD, Baker KB, Lowe MJ, Tkach JA, Cooper SE, Kopell BH, et al. Parkinson disease: pattern of functional MR imaging activation during deep brain stimulation of subthalamic nucleus–initial experience. Radiology 2006;239(1):209–16.
[8] Kahan J, Mancini L, Urner M, Friston K, Hariz M, Holl E, et al. Therapeutic subthalamic nucleus deep brain stimulation reverses cortico-thalamic coupling during voluntary movements in Parkinson's disease. PloS One 2012;7(12):e50270.
[9] Paschali A, Constantoyannis C, Angelatou F, Vassilakos P. Perfusion brain SPECT in assessing motor improvement after deep brain stimulation in Parkinson's disease. Acta Neurochir 2013;155(3):497–505.
[10] Min HK, Hwang SC, Marsh MP, Kim I, Knight E, Striemer B, et al. Deep brain stimulation induces BOLD activation in motor and non-motor networks: an fMRI comparison study of STN and EN/GPi DBS in large animals. Neuroimage 2012;63(3):1408–20.
[11] Knight EJ, Min HK, Hwang SC, Marsh MP, Paek S, Kim I, et al. Nucleus accumbens deep brain stimulation results in insula and prefrontal activation: a large animal FMRI study. PloS One 2013;8(2):e56640.
[12] Kim JP, Min HK, Knight EJ, Duffy PS, Abulseoud OA, Marsh MP, et al. Centromedian-parafascicular deep brain stimulation induces differential functional inhibition of the motor, associative, and limbic circuits in large animals. Biol Psychiatry 2013;74(12):917–26.
[13] Benarroch EE. Subthalamic nucleus and its connections: Anatomic substrate for the network effects of deep brain stimulation. Neurology 2008;70(21):1991–5.
[14] Herzog J, Fietzek U, Hamel W, Morsnowski A, Steigerwald F, Schrader B, et al. Most effective stimulation site in subthalamic deep brain stimulation for Parkinson's disease. Mov Disord 2004;19(9):1050–4.
[15] Lunsford LD, Martinez AJ, Latchaw RE. Stereotaxic surgery with a magnetic resonance- and computerized tomography-compatible system. J Neurosurg 1986;64(6):872–8.
[16] Saleem KSL, Logothetis NK. Atlas of the rhesus monkey brain. London: Academic Press; 2007.
[17] Lozano AM, Dostrovsky J, Chen R, Ashby P. Deep brain stimulation for Parkinson's disease: disrupting the disruption. Lancet Neurol 2002;1(4):225–31.
[18] DeLong M, Wichmann T. Deep brain stimulation for movement and other neurologic disorders. Ann N Y Acad Sci 2012;1265:1–8.
[19] Haslinger B, Boecker H, Buchel C, Vesper J, Tronnier VM, Pfister R, et al. Differential modulation of subcortical target and cortex during deep brain stimulation. Neuroimage 2003;18(2):517–24.
[20] Asanuma K, Tang C, Ma Y, Dhawan V, Mattis P, Edwards C, et al. Network modulation in the treatment of Parkinson's disease. Brain 2006;129(Pt 10):2667–78.
[21] Kalbe E, Voges J, Weber T, Haarer M, Baudrexel S, Klein JC, et al. Frontal FDG-PET activity correlates with cognitive outcome after STN-DBS in Parkinson disease. Neurology 2009;72(1):42–9.
[22] Fraix V, Pollak P, Vercueil L, Benabid AL, Mauguiere F. Effects of subthalamic nucleus stimulation on motor cortex excitability in Parkinson's disease. Clin Neurophysiol 2008;119(11):2513–8.
[23] Grafton ST, Turner RS, Desmurget M, Bakay R, Delong M, Vitek J, et al. Normalizing motor-related brain activity: subthalamic nucleus stimulation in Parkinson disease. Neurology 2006;66(8):1192–9.
[24] Gradinaru V, Mogri M, Thompson KR, Henderson JM, Deisseroth K. Optical deconstruction of parkinsonian neural circuitry. Science 2009;324(5925):354–9.
[25] Devergnas A, Wichmann T. Cortical potentials evoked by deep brain stimulation in the subthalamic area. Front Syst Neurosci 2011;5:30.
[26] Brunenberg EJ, Moeskops P, Backes WH, Pollo C, Cammoun L, Vilanova A, et al. Structural and resting state functional connectivity of the subthalamic nucleus: identification of motor STN parts and the hyperdirect pathway. PloS One 2012;7(6):e39061.
[27] Hirschmann J, Ozkurt TE, Butz M, Homburger M, Elben S, Hartmann CJ, et al. Distinct oscillatory STN-cortical loops revealed by simultaneous MEG and local field potential recordings in patients with Parkinson's disease. Neuroimage 2011;55(3):1159–68.
[28] Li Q, Ke Y, Chan DC, Qian ZM, Yung KK, Ko H, et al. Therapeutic deep brain stimulation in Parkinsonian rats directly influences motor cortex. Neuron 2012;76(5):1030–41.
[29] Kumar R, Lozano AM, Sime E, Halket E, Lang AE. Comparative effects of unilateral and bilateral subthalamic nucleus deep brain stimulation. Neurology 1999;53(3):561–6.
[30] Parent A, Hazrati LN. Functional anatomy of the basal ganglia. I. The cortico-basal ganglia-thalamo-cortical loop. Brain Res Brain Res Rev 1995;20(1):91–127.
[31] Parent A, Hazrati LN. Functional anatomy of the basal ganglia. II. The place of subthalamic nucleus and external pallidum in basal ganglia circuitry. Brain Res Brain Res Rev 1995;20(1):128–54.
[32] Chopra A, Tye SJ, Lee KH, Matsumoto J, Klassen B, Adams AC, et al. Voltage-dependent mania after subthalamic nucleus deep brain stimulation in Parkinson's disease: a case report. Biol Psychiatry 2011;70(2):e5–7.
[33] Mallet L, Schupbach M, N'Diaye K, Remy P, Bardinet E, Czernecki V, et al. Stimulation of subterritories of the subthalamic nucleus reveals its role in the integration of the emotional and motor aspects of behavior. Proc Natl Acad Sci U S A 2007;104(25):10661–6.
[34] Frankemolle AM, Wu J, Noecker AM, Voelcker-Rehage C, Ho JC, Vitek JL, et al. Reversing cognitive-motor impairments in Parkinson's disease patients using a computational modelling approach to deep brain stimulation programming. Brain 2010;133(Pt 3):746–61.
[35] Hill KK, Campbell MC, McNeely ME, Karimi M, Ushe M, Tabbal SD, et al. Cerebral blood flow responses to dorsal and ventral STN DBS correlate with gait and balance responses in Parkinson's disease. Exp Neurol 2013;241:105–12.
[36] Weise LM, Seifried C, Eibach S, Gasser T, Roeper J, Seifert V, et al. Correlation of active contact positions with the electrophysiological and anatomical subdivisions of the subthalamic nucleus in deep brain stimulation. Stereotact Funct Neurosurg 2013;91(5):298–305.
[37] Alexander GE, DeLong MR, Strick PL. Parallel organization of functionally segregated circuits linking basal ganglia and cortex. Annu Rev Neurosci 1986;9:357–81.
[38] Volkmann J, Daniels C, Witt K. Neuropsychiatric effects of subthalamic neurostimulation in Parkinson disease. Nat Rev Neurol 2010;6(9):487–98.
[39] Stefani A, Lozano AM, Peppe A, Stanzione P, Galati S, Tropepi D, et al. Bilateral deep brain stimulation of the pedunculopontine and subthalamic nuclei in severe Parkinson's disease. Brain 2007;130(Pt 6):1596–607.
[40] Neagu B, Tsang E, Mazzella F, Hamani C, Moro E, Hodaie M, et al. Pedunculopontine nucleus evoked potentials from subthalamic nucleus stimulation in Parkinson's disease. Exp Neurol 2013;250:221–7.